The fusion kinase ITK-SYK mimics a T cell receptor signal and drives oncogenesis in conditional mouse models of peripheral T cell lymphoma

Konstanze Pechloff,[1] Julian Holch,[1] Uta Ferch,[1] Marc Schweneker,[1] Kristina Brunner,[1] Markus Kremer,[2] Tim Sparwasser,[3] Leticia Quintanilla-Martinez,[4,5] Ursula Zimber-Strobl,[7] Berthold Streubel,[8] Andreas Gewies,[1,6] Christian Peschel,[1] and Jürgen Ruland[1,6]

[1]Third Medical Department, Technical University of Munich, Klinikum rechts der Isar, [2]Institute of Pathology, and [3]Institute of Medical Microbiology, Immunology and Hygiene, Technical University of Munich, 81675 Munich, Germany
[4]Institute of Pathology, Eberhard Karls University Tübingen, 72076 Tübingen, Germany
[5]Institute of Pathology and [6]Laboratory of Signaling in the Immune System, Helmholtz Zentrum München German Research Center for Environmental Health, 85764 Neuherberg, Germany
[7]Department of Gene Vectors, Helmholtz Zentrum München German Research Center for Environmental Health, 81377 Munich, Germany
[8]Department of Pathology, Medical University of Vienna, 1090 Vienna, Austria

Peripheral T cell lymphomas (PTCLs) are highly aggressive malignancies with poor prognosis. Their molecular pathogenesis is not well understood and small animal models for the disease are lacking. Recently, the chromosomal translocation t(5;9)(q33;q22) generating the interleukin-2 (IL-2)–inducible T cell kinase (ITK)–spleen tyrosine kinase (SYK) fusion tyrosine kinase was identified as a recurrent event in PTCL. We show that ITK-SYK associates constitutively with lipid rafts in T cells and triggers antigen-independent phosphorylation of T cell receptor (TCR)–proximal proteins. These events lead to activation of downstream pathways and acute cellular outcomes that correspond to regular TCR ligation, including up-regulation of CD69 or production of IL-2 in vitro or deletion of thymocytes and activation of peripheral T cells in vivo. Ultimately, conditional expression of patient-derived ITK-SYK in mice induces highly malignant PTCLs with 100% penetrance that resemble the human disease. Our work demonstrates that constitutively enforced antigen receptor signaling can, in principle, act as a powerful oncogenic driver. Moreover, we establish a robust clinically relevant and genetically tractable model of human PTCL.

CORRESPONDENCE
Jürgen Ruland:
jruland@lrz.tu-muenchen.de

Abbreviations used: DP, double positive; eGFP, enhanced GFP; IRES, internal ribosomal entry site; ITK, IL-2–inducible T cell kinase; PH, pleckstrin homology; PTCL, peripheral T cell lymphoma; SH, Src homology; SP, single positive; SYK, spleen tyrosine kinase; TH, TEC homology.

Peripheral T cell lymphomas (PTCLs) belong to the category of the most aggressive non-Hodgkin's lymphomas with a high mortality rate, minimal effectiveness of conventional chemotherapy, and only 10–30% long-term survivors (Savage, 2007). PTCLU (PTCL unspecified) represents the largest PTCL subtype, and most patients present with advanced disease and frequent involvement of extranodal sites including spleen, bone marrow, liver, or blood. Pathologically, there is usually a diffuse infiltrate of atypical large T cells that exhibit an activated phenotype and a gene expression signature that resembles that of activated T cells (Piccaluga et al., 2007). Although PTCLs have a worse prognosis than aggressive B cell lymphomas, they are still largely treated the same way because rational treatment strategies for PTCL are currently missing (Escalón et al., 2005). The development of such strategies requires a better understanding of the molecular PTCL pathogenesis and, in addition, preclinical animal models for the human disease.

The chromosomal translocation t(5;9)(q33;q22) was recently identified as a recurrent

Tim Sparwasser's present address is Institute of Infection Immunology, TWINCORE, Centre for Experimental and Clinical Infection Research, 30625 Hannover, Germany.

The Rockefeller University Press $30.00
J. Exp. Med. Vol. 207 No. 5 1031-1044
www.jem.org/cgi/doi/10.1084/jem.20092042

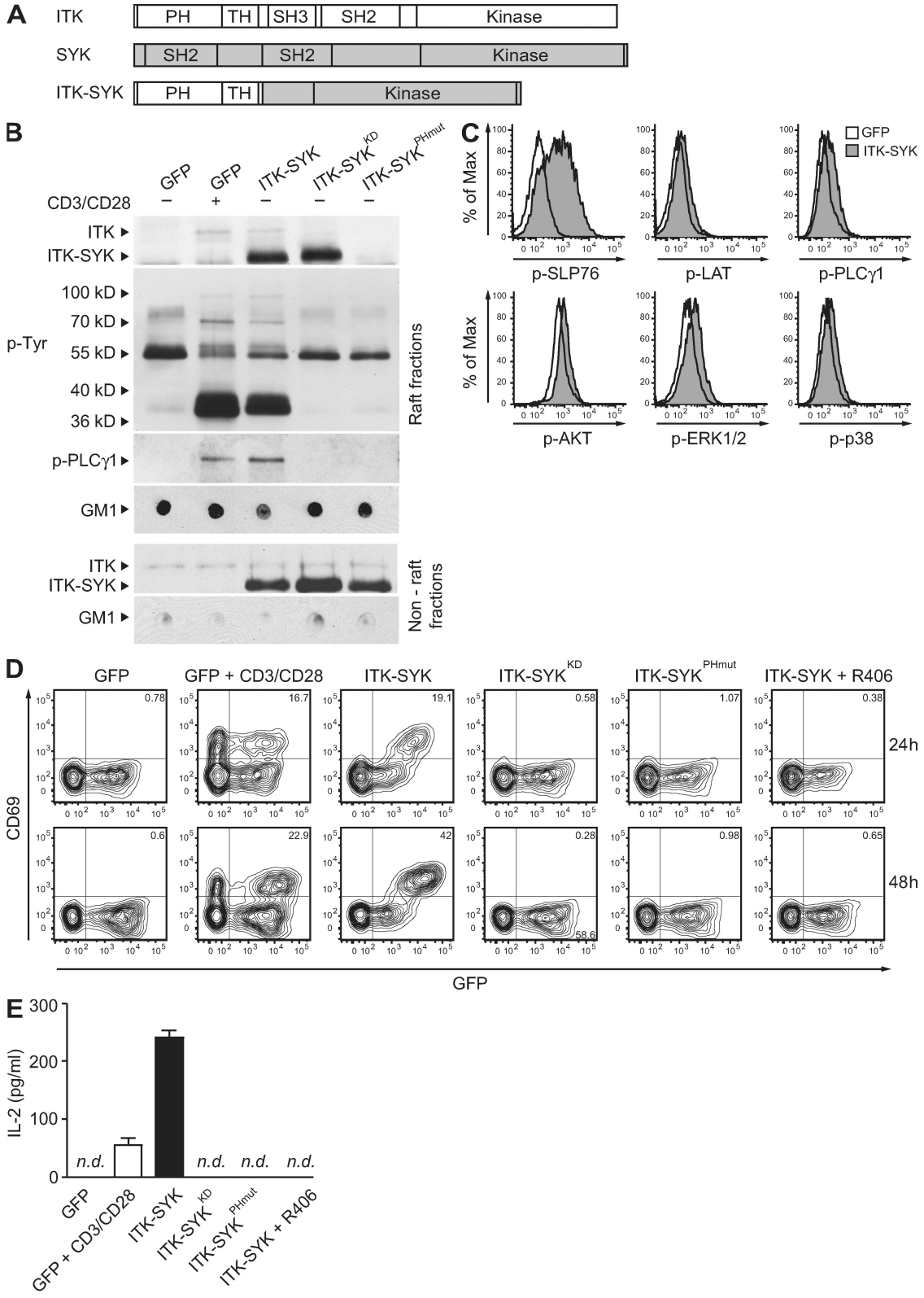

Figure 1. ITK-SYK mimics a TCR signal in vitro. (A) Schematic representations of ITK, SYK, and ITK-SYK. Kinase, tyrosine kinase domain. See text for details. (B) Constitutive ITK-SYK signaling in T cell lipid rafts. Jurkat cells were infected with retroviruses carrying ITK-SYK, ITK-SYK^{KD}, ITK-SYK^{PHmut} together with GFP (ITK-SYK, ITK-SYK^{KD}, or ITK-SYK^{PHmut}), or GFP only as a control (GFP). Lipid raft fractions from unstimulated or anti-CD3– (5 µg/ml) and anti-CD28 (1 µg/ml)–stimulated cells were prepared and subjected to Western blot analysis with antibodies against ITK (top), phospho-tyrosine (p-Tyr), or phosphorylated

and specific genomic alteration in PTCLU (Streubel et al., 2006). This translocation fuses the *IL-2–inducible T cell kinase* (*ITK*) and the *spleen tyrosine kinase* (*SYK*) genes. ITK and SYK are both required for normal antigen-induced lymphocyte activation. ITK is the predominant TEC kinase family member expressed in T cells (Berg et al., 2005). It possesses an amino-terminal pleckstrin homology (PH) domain for plasma membrane recruitment, a TEC homology (TH) domain, Src homology (SH) 3 and SH2 domains for association with T cell adapter proteins, and a kinase domain for TCR downstream signaling (Fig. 1 A). SYK is highly expressed in B lymphocytes and myeloid cells, where it plays essential roles for immune cell activation (Sada et al., 2001). It is also expressed in developing thymocytes (Palacios and Weiss, 2007). SYK contains tandem SH2 domains for ligand-induced association with the BCR or other ITAM (immunoreceptor tyrosine-based activation motif)–containing immunoreceptors and a kinase domain for the phosphorylation of receptor-proximal molecules and subsequent signal transduction (Fig. 1 A).

The translocation t(5;9)(q33;q22) fuses the PH and TH regions from ITK to the SYK kinase domain (Fig. 1 A; Streubel et al., 2006). However, the molecular and cellular consequences of ITK-SYK expression in lymphocytes are unknown. In this paper, we show that ITK-SYK is a catalytically active tyrosine kinase that constitutively engages the antigen receptor signaling machinery in T cells. Conditional expression of ITK-SYK in vivo induces highly aggressive T cell lymphomas with 100% penetrance and clinical and pathological features of the human PTCL. This work demonstrates that constitutively enforced antigen receptor signaling can act as a strong oncogenic driver in lymphoma pathogenesis and establishes a clinically relevant mouse model of human PTCL.

RESULTS

ITK-SYK is a lipid raft–associated tyrosine kinase that mimics a TCR signal

To study the role of ITK-SYK in lymphomagenesis, we isolated an ITK-SYK fusion transcript from a human tumor specimen harboring the t(5;9)(q33;q22) translocation (Streubel et al., 2006) and generated retroviral expression vectors that coexpress different ITK-SYK versions together with a GFP. In vitro kinase assays revealed that patient-derived ITK-SYK is an active tyrosine kinase (unpublished data). Exchange of lysine to arginine in the ATP binding pocket of the kinase domain (K262R; equivalent to K402R in wild-type SYK) resulted in a catalytically inactive ITK-SYK^{KD} (kinase defective) version (unpublished data). To investigate functional roles of the ITK-SYK PH domain, we also introduced a point mutation into its lipid binding pocket by exchanging arginine 29 to cysteine (R29C; ITK-SYK^{PHmut}). This mutation corresponds to the previously characterized R29C mutation in the PH domain of wild-type ITK that interferes with ITK membrane recruitment (Bunnell et al., 2000).

First, we transduced ITK-SYK and its variants into Jurkat cells to study effects on T cell signal transduction (Abraham and Weiss, 2004; Fig. 1 B). As a control, we used Jurkat cells that had been infected with a retrovirus expressing only GPF. Western blotting with an ITK-specific antibody demonstrated strong and constitutive expression of ITK-SYK and ITK-SYK^{KD} in lipid rafts (Fig. 1 B). These are the subcellular fractions containing the membrane microdomains where TCR signaling is initiated (Dykstra et al., 2003). In contrast, the ITK-SYK^{PHmut} version does as expected not associate with lipid rafts, although it is expressed in the nonraft fractions at a similar level to that of ITK-SYK or ITK-SYK^{KD}.

In ITK-SYK–expressing cells, we detected tyrosine phosphorylation of several lipid raft–associated proteins including tyrosine phosphorylation of the TCR signal transducer PLCγ1 (Samelson, 2002). The pattern of tyrosine phosphorylation was similar to that of control Jurkat cells after stimulation with agonistic anti-CD3 and anti-CD28 antibodies to trigger antigen receptor signaling. Moreover, we observed a recruitment of endogenous ITK into the lipid rafts of ITK-SYK–expressing T cells as well as into rafts of cells that were stimulated via their TCR and CD28. In contrast, Jurkat cells that were transduced with ITK-SYK^{KD} or ITK-SYK^{PHmut} cells did not recruit ITK into lipid rafts and did not exhibit protein tyrosine phosphorylation above baseline. (Fig. 1 B).

Normal TCR signaling in Jurkat cells induces phosphorylation of the TCR-proximal adapters SLP-76 and LAT and subsequent activation of several downstream pathways, leading to the up-regulation of the activation marker CD69 and production of IL-2 (Samelson, 2002; Abraham and Weiss, 2004). To further study ITK-SYK signaling, we used intracellular flow cytometry with activation-specific antibodies directed against phosphorylated TCR signaling molecules (phosflow; Fig. 1 C). Constitutive ITK-SYK expression triggers tyrosine phosphorylation of SLP-76 and LAT. Again, PLC-γ1 phosphorylation was also detected. Moreover, we observed

PLCγ1 (p-PLCγ1). Dot blots with the lipid raft marker GM1 confirm equal loading. Data shown are representative of at least two independent experiments. (C) Phosflow analysis of ITK-SYK signaling. Jurkat cells were infected with ITK-SYK together with GFP or GFP only expressing retrovirus and intracellularly stained with activation-specific anti-phospho antibodies directed against the indicated T cell signaling molecules. Signaling was analyzed within the infected viable GFP$^+$ populations. Data shown are representative of four independent experiments. (D) ITK-SYK triggers kinase and PH domain–dependent T cell activation. Jurkat cells were infected as in B, left unstimulated, stimulated with 10 µg/ml anti-CD3 and 2 µg/ml anti-CD28, or treated with 2 µM R406 as indicated and analyzed by FACS. The percentage of infected GFP$^+$ CD69-expressing cells from unstimulated, stimulated, or R406-treated cells is indicated. Data shown are representative of five independent experiments. (E) ITK-SYK induces kinase and PH domain–dependent IL-2 production. Jurkat cells were infected as in B. Cells were left unstimulated, stimulated with 10 µg/ml anti-CD3 and 2 µg/ml anti-CD28, or treated with 2 µM R406 as indicated. IL-2 concentrations in the cell supernatants were determined by ELISA. Shown are the mean ± SD from triplicate samples. Data shown are representative of four independent experiments.

constitutive activation of the AKT, ERK, and p38 MAP kinase downstream pathways in ITK-SYK–expressing cells. The protein phosphorylation pattern correlated to that of control cells that were acutely stimulated with CD3 and CD28 antibodies (Fig. S1).

As cellular readouts for ITK-SYK function, we then monitored CD69 expression and IL-2 production (Fig. 1, D and E). Strong up-regulation of CD69 was detected in ITK-SYK–expressing cells, as well as in CD3/CD28-stimulated cells, but not in noninfected cells or cells infected with a GFP control virus (Fig. 1 D). The up-regulation of CD69 by ITK-SYK was dependent on both an intact kinase domain and an intact PH domain because ITK-SYK^{KD} or ITK-SYK^{PHmut} versions did not enhance CD69 expression.

ITK-SYK also triggered a profound production of IL-2, which was even higher than the IL-2 production induced by optimal CD3/CD28 costimulation with agonistic antibodies (Fig. 1 E). Similar to the up-regulation of CD69, the ITK-SYK–induced secretion of IL-2 required an intact ITK-SYK kinase and PH domain.

To investigate the importance of ITK-SYK kinase activity in an alternative way, we also tested whether ITK-SYK signaling might be sensitive to small molecule inhibition. To this end, we used the immunosuppressant wild-type SYK inhibitor R406

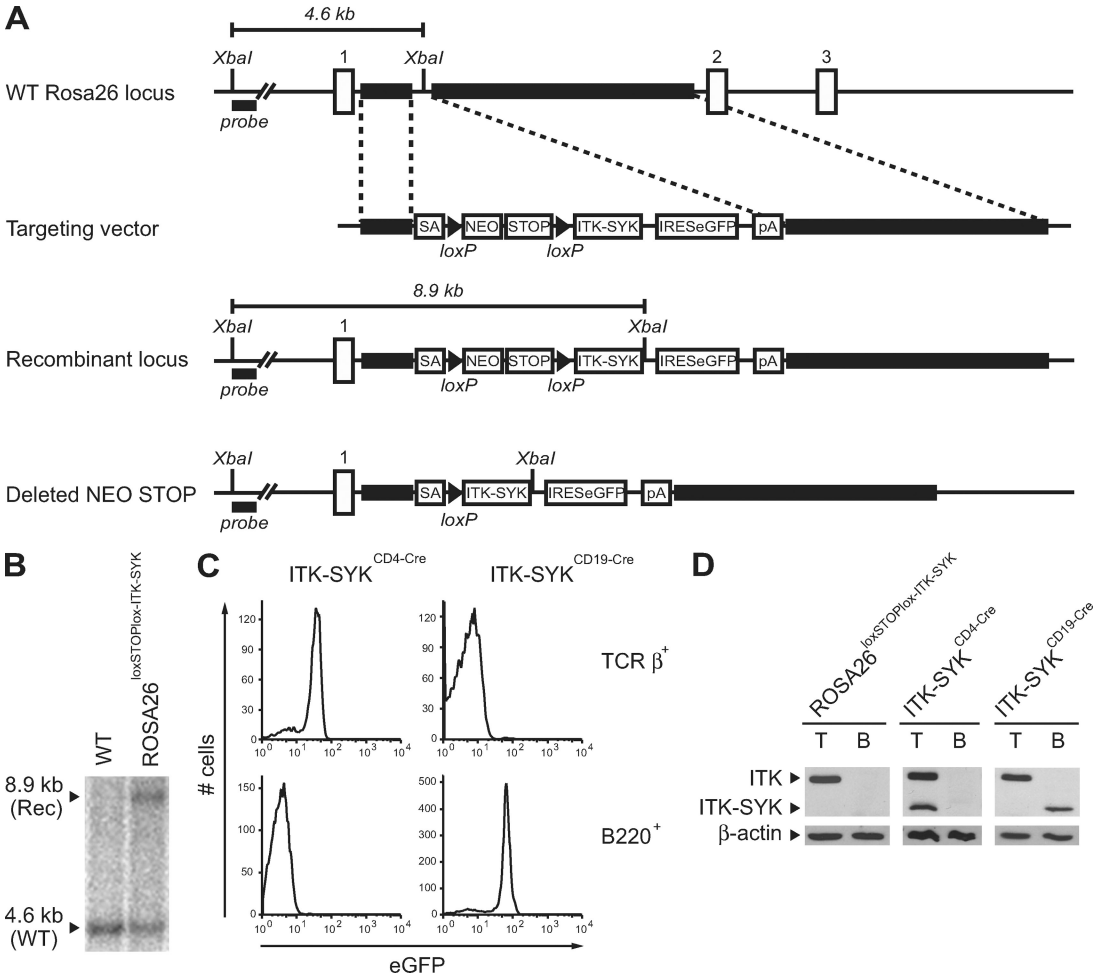

Figure 2. A mouse model for conditional ITK-SYK expression. (A) Schematic representation of the gene-targeting strategy. A targeting vector that carries the human ITK-SYK cDNA together with an IRES eGFP sequence preceded by a loxP-flanked NEO-STOP cassette was constructed and used to generate Rosa26$^{loxSTOPlox\text{-}ITK\text{-}SYK}$ mice as described in Materials and methods. The recombinant Rosa26 locus and the ITK-SYK–expressing locus upon Cre-mediated deletion of the NEO-STOP cassette are indicated. SA, splice acceptor site; pA, polyA sequence; 1–3, Rosa26 exon 1–3; probe, flanking probe for Southern blot analysis. (B) Southern blot analysis. Genomic DNA from a wild-type (WT) and a successfully targeted Rosa26$^{loxSTOPlox\text{-}ITK\text{-}SYK}$ embryonic stem cell clone was digested with XbaI and Southern blotted with the flanking probe indicated in A. Sizes of the wild-type and recombinant (Rec) fragments are indicated. (C) Conditional expression of ITK-SYK in T and B cells in vivo. ROSA26$^{loxSTOPlox\text{-}ITK\text{-}SYK}$ mice were crossed to CD4-Cre or CD19-Cre transgenic mice for T or B cell–specific ITK-SYK expression. Peripheral lymphocyte suspensions of double transgenic 5-wk-old ITK-SYK$^{CD4\text{-}Cre}$ or ITK-SYK$^{CD19\text{-}Cre}$ mice were stained against TCR-β or B220. eGFP fluorescence indicative of ITK-SYK expression in the TCR-β$^+$ T cells or B220$^+$ B cells of the respective animals was analyzed using FACS. Data shown are representative of >40 mice per genotype analyzed. (D) Western blot analysis of conditional ITK-SYK expression. Individual mature T and B cell populations from 5-wk-old Rosa26$^{loxSTOPlox\text{-}ITK\text{-}SYK}$, ITK-SYK$^{CD4\text{-}Cre}$, and ITK-SYK$^{CD19\text{-}Cre}$ mice were sorted with magnetic beads and subjected to Western blot analysis with an anti-ITK antibody. Bands of wild-type ITK and ITK-SYK are indicated. Western blotting for β-actin demonstrated equal protein loading. Data shown are representative of five independent experiments.

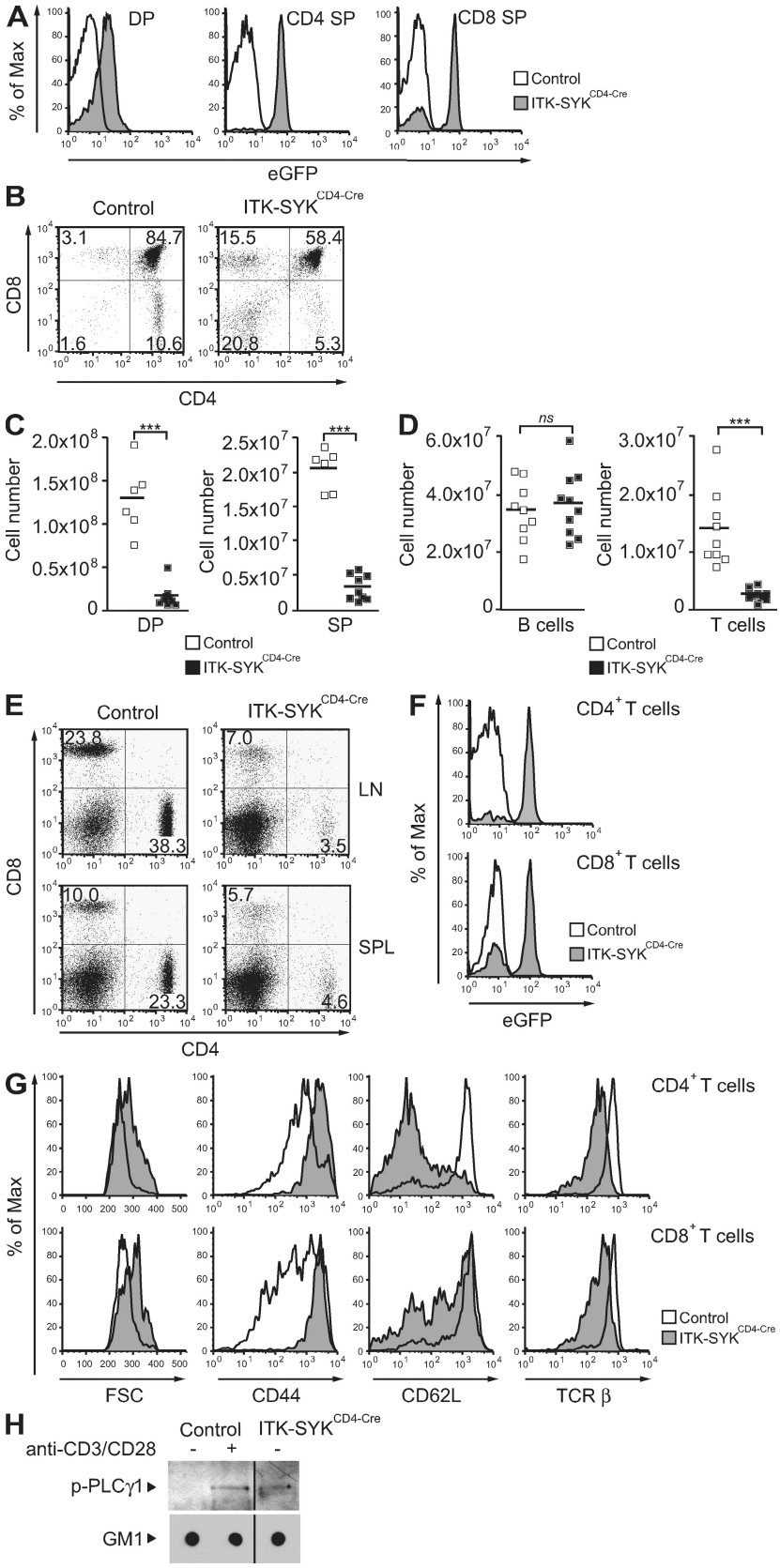

Figure 3. ITK-SYK mimics a TCR signal in vivo. (A) ITK-SYK expression in the thymus of ITK-SYK$^{CD4\text{-}Cre}$ animals. Thymocytes were stained against CD4 and CD8 and analyzed by FACS. eGFP fluorescence indicative of ITK-SYK expression was measured in the CD4$^+$CD8$^+$ DP and in the CD4$^+$ or CD8$^+$ SP populations of 4–5-wk-old ITK-SYK$^{CD4\text{-}Cre}$ or control (CD4-Cre transgenic) mice. (B and C) ITK-SYK induces DP thymocyte deletion. (B) Thymocytes were stained as in A and analyzed for the expression of CD4 or CD8. The frequencies of individual thymocyte subsets are indicated. (C) The total DP or SP thymocyte cell numbers from ITK-SYK$^{CD4\text{-}Cre}$ (n = 9) or control (n = 6) mice are shown. (D) Total splenic B or T cell numbers from ITK-SYK$^{CD4\text{-}Cre}$ (n = 10) or control (n = 9) mice are indicated. Each symbol in C and D represents an individual mouse. Statistical significance was analyzed using the unpaired two-tailed Student's t test. ***, statistically significant ($P < 0.0001$); *ns*, not statistically significant ($P \geq 0.05$). Horizontal bars indicate the means. (E and F) Single cell suspensions from lymph node (LN) or spleen (SPL) from 4–5-wk-old ITK-SYK$^{CD4\text{-}Cre}$ or control mice were stained against CD4 and CD8. (E) CD4 and CD8 expression was analyzed by FACS. The frequencies of individual T cell subsets are indicated. (F) eGFP fluorescence indicative of ITK-SYK expression was determined in peripheral CD4$^+$ or CD8$^+$ T cells of ITK-SYK$^{CD4\text{-}Cre}$ or control mice. Data from spleen are shown. (G) ITK-SYK expressing T cells exhibit an activated phenotype in vivo. Peripheral lymphocytes from 4–5-wk-old ITK-SYK$^{CD4\text{-}Cre}$ or control mice were stained against CD4, CD8, CD44, CD62L, and TCR-β. Forward scattering (FCS) as a parameter for cell size and expression of CD44, CD62L, and TCR-β was analyzed in the CD4$^+$ and CD8$^+$ T cell compartments using FACS. Data shown in A, B, and E–G are representative of five independent experiments with a total number of at least 10 mice analyzed per genotype. (H) ITK-SYK induces PLCγ1 phosphorylation in primary T cells in vivo. Splenic T cells were isolated from control or ITK-SYK$^{CD4\text{-}Cre}$ mice that were >12 wk old. Cells were left unstimulated and control cells additionally stimulated with 5 µg/ml of anti-CD3 and 1 µg/ml of anti-CD28. Lipid raft fractions were prepared and subjected to Western blot analysis with an anti–phospho-PLCγ1 antibody. Dot blots for GM1 show successful raft preparation and equal loading. Data shown are representative of three independent experiments. Black lines indicate that intervening lanes have been spliced out.

which is currently in clinical trails for inflammatory, autoimmune, and selected malignant diseases (Weinblatt et al., 2008; Friedberg et al., 2010). Both ITK-SYK–induced up-regulation of CD69 and IL-2 production were completely blocked by R406 treatment (Fig. 1, D and E).

Together, these first in vitro experiments indicate that ITK-SYK is a lipid raft–associated tyrosine kinase, which constitutively engages molecular components of the TCR signaling machinery and thereby mimics aspects of a TCR signal in the absence of a ligand. Because an SYK kinase inhibitor or inactivating mutations in the ITK-SYK kinase or PH domain block ITK-SYK signaling, we additionally conclude that both kinase activity and membrane recruitment are essential for productive ITK-SYK signal transduction.

A mouse model for conditional ITK-SYK expression

Based on the association of ITK-SYK with human PTCLs, we particularly wanted to study the effects of ITK-SYK signaling in lymphocytes in vivo. To this end, we created a novel mouse model that allows ITK-SYK expression in a controlled and inducible fashion (Fig. 2). We introduced a human ITK-SYK fusion cDNA preceded by a loxP-flanked transcriptional and translational STOP cassette into the ubiquitously expressed Rosa26 locus using previously established gene targeting (Sasaki et al., 2006; Fig. 2, A and B). The resulting Rosa26$^{loxSTOPlox\text{-}ITK\text{-}SYK}$ mice were crossed to CD4-Cre transgenic animals (Lee et al., 2001) to induce T cell–specific excision of the STOP cassette and T cell–restricted ITK-SYK expression in the Rosa26$^{loxSTOPlox\text{-}ITK\text{-}SYK}$ × CD4-Cre double

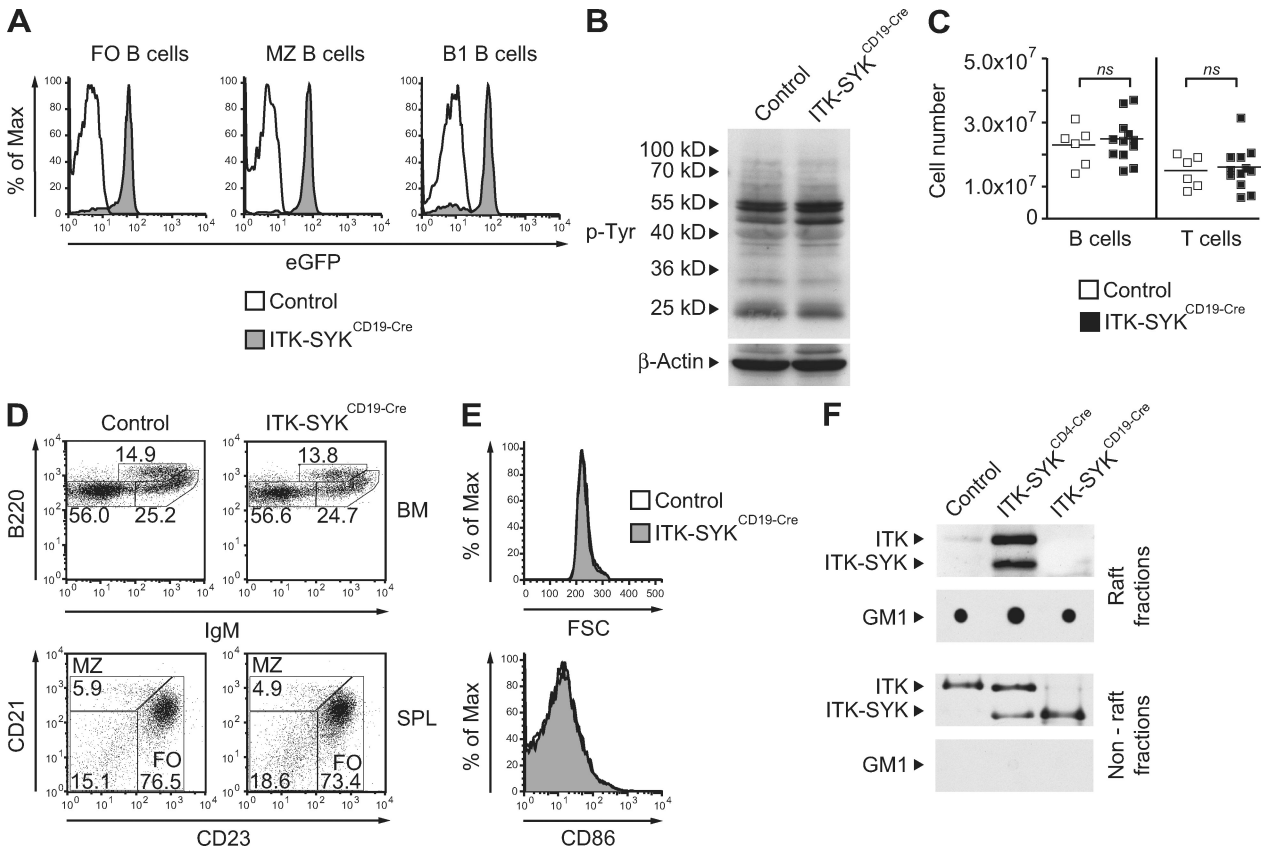

Figure 4. B cell–intrinsic ITK-SYK expression does not affect B cell development or activation. (A) Single cell suspensions from the spleens or peritoneal cavities of ITK-SYK$^{CD19\text{-}Cre}$ or control (CD19-Cre) mice were stained against B220, CD21, CD23, and CD5. eGFP fluorescence indicative of ITK-SYK expression was determined in the splenic follicular (FO), splenic marginal zone (MZ), or peritoneal B1 B cell compartments using FACS. (B) Cytoplasmic extracts of purified mature B cells from 5-wk-old control or ITK-SYK$^{CD19\text{-}Cre}$ mice were subjected to Western blot analysis with an antibody against phospho–tyrosine (p-Tyr). Western blotting for β-actin demonstrated equal protein loading. Data shown are representative of three independent experiments. (C) Total splenic B or T cell numbers from ITK-SYK$^{CD19\text{-}Cre}$ (n = 12) or control (n = 6) mice are shown. Each symbol represents an individual mouse. Statistical significance was analyzed using the unpaired two-tailed Student's t test. *ns*, non–statistically significant differences ($P \geq 0.05$). Horizontal bars indicate the means. (D) Lymphocyte preparations from bone marrow (BM) or spleen (SPL) of ITK-SYK$^{CD19\text{-}Cre}$ or control mice were stained against B220, IgM, CD21, or CD23 and analyzed by FACS. The percentages of individual B cell populations are indicated. FO, follicular B cells; MZ, marginal zone B cells. (E) Forward scattering (FCS) and expression of CD86 was analyzed on B220^{+} mature B cells from ITK-SYK$^{CD19\text{-}Cre}$ or control mice using FACS. Data shown in A and C–E are representative of four independent experiments with total numbers of at least six 5–7-wk-old mice per genotype analyzed. (F) ITK-SYK is constitutively associated with T but not with B cell lipid rafts. Lipid raft and nonraft fractions were prepared from purified splenic T cells of control or ITK-SYK$^{CD4\text{-}Cre}$ mice or from mature B cells of ITK-SYK$^{CD19\text{-}Cre}$ mice that were >12 wk old. The fractions were subsequently analyzed for the presence of ITK or ITK-SYK by Western blot analysis using an antibody against ITK. Dot blots for GM1 show successful raft preparation and equal loading. Data shown are representative of three independent experiments.

transgenic offspring (from now on called ITK-SYK$^{CD4\text{-}Cre}$ mice). As Cre-catalyzed recombination also induces enhanced GFP (eGFP) expression from an internal ribosomal entry site (IRES), we can visualize ITK-SYK–expressing cells. To induce ITK-SYK expression in the B cell lineage, we crossed the Rosa26$^{loxSTOPlox\text{-}ITK\text{-}SYK}$ line with CD19-Cre transgenic animals (Rickert et al., 1997; double-transgenic offspring called ITK-SYK$^{CD19\text{-}Cre}$ mice). FACS analysis in 5-wk-old animals revealed specific expression of the recombined ITK-SYK allele in >85% of peripheral T cells of ITK-SYK$^{CD4\text{-}Cre}$ mice or B cells in ITK-SYK$^{CD19\text{-}Cre}$ mice (Fig. 2 C). Expression of the ITK-SYK protein in the respective lymphocyte lineages was confirmed by Western blotting (Fig. 2 D).

ITK-SYK can imitate a TCR but not a BCR signal in vivo

We first focused on lymphocyte development in young (4–5-wk-old) animals. The CD4-Cre transgene mediates loxP recombination at the CD4$^+$CD8$^+$ double-positive (DP) stage of thymocyte development and continues in single-positive (SP) cells (Lee et al., 2001). The DP stage is the period of T cell differentiation, when thymocytes expressing autoreactive TCRs receive strong TCR signals and are subsequently deleted by negative selection to prevent autoimmunity (Sebzda et al., 1999). As expected, ITK-SYK expression was observed at the DP stage in ITK-SYK$^{CD4\text{-}Cre}$ mice (Fig. 3 A), leading to a profound reduction in the frequencies and absolute numbers of DP thymocytes in these animals (Fig. 3, B and C). These findings are consistent with the hypothesis that ITK-SYK imitates features of a strong TCR signal, as observed in our in vitro experiments in Fig. 1. The decrease in DP cells is followed by a diminishment of the SP populations (Fig. 3 C) and reduced numbers (Fig. 3 D) and frequencies (Fig. 3 E) of mature peripheral T cells. Still, the majority of the peripheral CD4$^+$ and CD8$^+$ T cells express the fusion kinase (Fig. 3 F; Fig. 2, C and D; and not depicted). These ITK-SYK–expressing CD4$^+$ and CD8$^+$ peripheral T cells exhibit an activated phenotype, which is characterized by a large cell size, high expression of the activation marker CD44, and low expression of CD62L (Fig. 3 G). Furthermore, these cells show down-regulated TCR-β surface expression. Histological in vivo analysis revealed that these activated T cells are highly proliferative but do not undergo apoptosis, as determined by Ki-67 immunohistochemistry and staining for active Caspase-3 (Fig. S2). Moreover, ITK-SYK–expressing T cells exhibit tyrosine phosphorylation of multiple lipid raft–associated proteins, including PLC-γ1, that is similar to wild-type T cells that are stimulated via the TCR with anti-CD3/CD28 antibodies (Fig. 3 H and not depicted). B cell development was not affected in ITK-SYK$^{CD4\text{-}Cre}$ mice (Fig. 3 D and not depicted).

To test whether B cell–intrinsic expression of ITK-SYK would influence B cell development or activation, we analyzed ITK-SYK$^{CD19\text{-}Cre}$ mice. In these animals, we observed an onset of B cell–specific ITK-SYK expression in the bone marrow and high percentages of ITK-SYK–expressing B cells in all peripheral B cell compartments including follicular, marginal zone, and B1 B cells (Fig. 4 A; Fig. 2, C and D; and not depicted). However, the overall protein tyrosine phosphorylation pattern did not differ between wild-type and ITK-SYK–expressing B lymphocytes (Fig. 4 B). Moreover, we did not detect any effects of B cell–intrinsic ITK-SYK expression on the total B cell

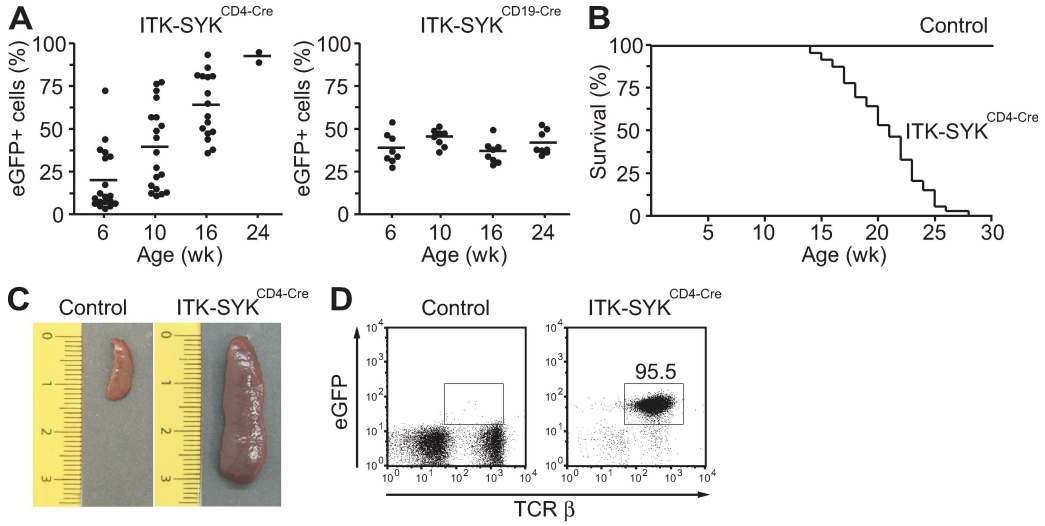

Figure 5. Conditional expression of ITK-SYK in T cells induces a lymphoproliferative disease. (A) Peripheral blood samples from ITK-SYK$^{CD4\text{-}Cre}$ (starting with $n = 19$) and ITK-SYK$^{CD19\text{-}Cre}$ mice ($n = 8$) were obtained at the indicated time points. The frequencies of eGFP fluorescent lymphocytes in individual animals were determined by FACS analysis. The total number of ITK-SYK$^{CD4\text{-}Cre}$ mice declined over time as a result of disease-related mortality. Horizontal bars indicate the means. (B) Kaplan-Meier curve of ITK-SYK$^{CD4\text{-}Cre}$ ($n = 73$) and control (CD4-Cre) mice ($n = 15$). (C) Macroscopic appearance of representative spleens from 20-wk-old control and ITK-SYK$^{CD4\text{-}Cre}$ mice are shown (in centimeters). (D) Splenocytes from 20-wk-old control and ITK-SYK$^{CD4\text{-}Cre}$ mice were stained with antibodies against TCR-β. The frequency of eGFP–expressing T cells in a diseased ITK-SYK$^{CD4\text{-}Cre}$ mouse is indicated. Data shown in C and D are representative of a total number of 20 mice per genotype analyzed.

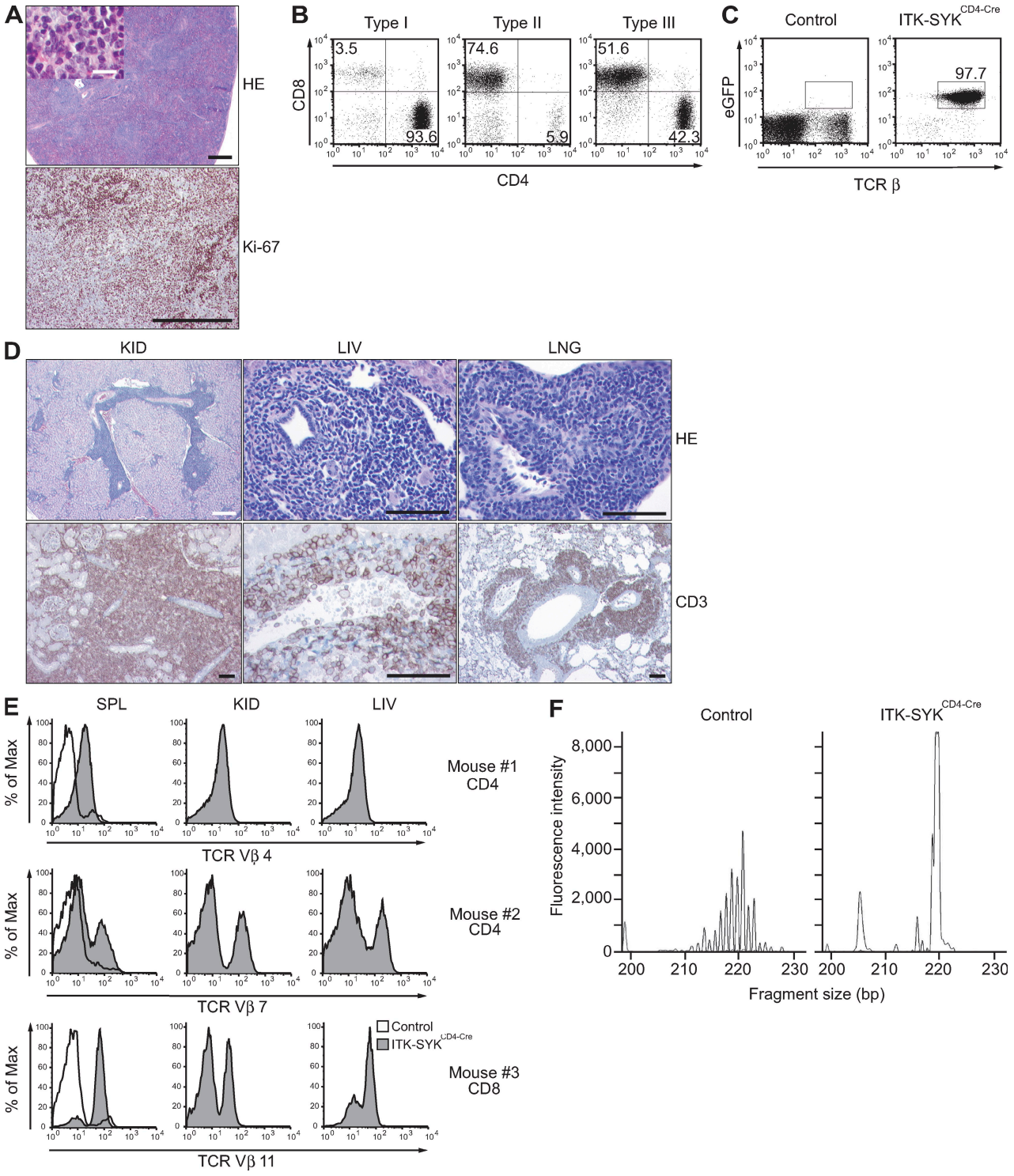

Figure 6. PTCL in ITK-SYK$^{CD4\text{-}Cre}$ mice. (A) Disruption of the splenic architecture with highly proliferative cells in ITK-SYK$^{CD4\text{-}Cre}$ mice was revealed by hematoxylin and eosin (H&E) staining and immunohistochemistry with anti–Ki-67 antibodies. Bars: (black) 1 mm; (white) 50 µm. Data shown are representative of five diseased ITK-SYK$^{CD4\text{-}Cre}$ mice analyzed. (B) Splenic cells from diseased ITK-SYK$^{CD4\text{-}Cre}$ mice were stained against CD4 and CD8 and analyzed by FACS. Selected examples of each type of T cell expansion from a total number of 40 mice analyzed are shown. (C) Bone marrow cell preparations from diseased ITK-SYK$^{CD4\text{-}Cre}$ or control (CD4-Cre) mice were stained with antibodies against TCR-β. The frequency of eGFP^{+} T cells is indicated. Data are representative of five independent experiments with a total number of 15 mice per genotype analyzed. (D) Solid organ infiltration of abnormal CD3^{+} T cells. Tissue sections from kidney (KID), liver (LIV), and lung (LNG) of affected ITK-SYK$^{CD4\text{-}Cre}$ animals were stained with H&E. Immunohistochemistry with anti-CD3 antibodies was additionally performed. Bars: (black) 200 µm; (white), 1 mm. Data shown are representative of five diseased ITK-SYK$^{CD4\text{-}Cre}$ mice

numbers (Fig. 4 C), the frequencies of individual B cell subsets (Fig. 4 D and not depicted), B cell size, or activation status (Fig. 4 E and not depicted). Thus, although the TCR and BCR share many molecular features of downstream signaling (Myung et al., 2000), enforced B cell–specific expression of ITK-SYK has apparently no overt effects on B cell biology.

We hypothesized that the fundamentally different functions of ITK-SYK in the T and B cell lineage could, in part, be the result of a cell type–specific localization of the fusion kinase into subcellular compartments because the protein region that is responsible for membrane recruitment originates from the T cell kinase ITK. Indeed, although T cells from ITK-SYK$^{CD4\text{-}Cre}$ mice and B cells from ITK-SYK$^{CD19\text{-}Cre}$ mice express similar amounts of ITK-SYK in cytoplasmic non-raft fractions, the association of ITK-SYK with lipid rafts is only observed in T and not in B cells (Fig. 4 F). Similar to that seen in Fig. 1 B, ITK-SYK expression in T cells also induces recruitment of wild-type ITK into lipid rafts. Thus, the combined analysis of ITK-SYK$^{CD4\text{-}Cre}$ and ITK-SYK$^{CD19\text{-}Cre}$ mice demonstrates that ITK-SYK mimics a strong antigen receptor signal in primary T cells but not in B cells in vivo. The results additionally indicate that ITK-SYK depends on an appropriate cellular microenvironment for productive signaling.

ITK-SYK expression in T cells induces a lymphoproliferative disease

To investigate potential oncogenic roles of ITK-SYK, we were especially interested in the long-term consequences of ITK-SYK expression in vivo. Therefore, we followed cohorts of ITK-SYK$^{CD4\text{-}Cre}$ (n = 19) and ITK-SYK$^{CD19\text{-}Cre}$ mice (n = 8) and regularly determined the frequencies of eGFP$^+$ ITK-SYK–expressing T or B cells in their peripheral blood (Fig. 5 A). The percentages of ITK-SYK–expressing T cells increased continuously in ITK-SYK$^{CD4\text{-}Cre}$ mice and rose up to almost 100%, indicating a profound T cell lymphoproliferative disorder. Starting at ~12 wk of age, the animals became overtly ill and eventually developed wasting and runting symptoms, lethargy, hunched postures, and distended abdomens. We had to sacrifice several mice from this series for ethical reasons. However, the medium frequency of ITK-SYK–expressing B cells in ITK-SYK$^{CD19\text{-}Cre}$ mice stayed constant during that time (Fig. 5 A).

Next, we obtained survival curves from ITK-SYK$^{CD4\text{-}Cre}$ (n = 73) and control mice (n = 15; Fig. 5 B). Although all ITK-SYK$^{CD4\text{-}Cre}$ animals succumbed to disease or had to be euthanized within 27 wk of age, the control mice did not develop any pathological symptoms.

ITK–SYK–expressing mice develop PTCL

To characterize the disease in ITK-SYK$^{CD4\text{-}Cre}$ mice in detail, we sacrificed animals at 20 wk of age or upon disease signs. All spleens of ITK-SYK$^{CD4\text{-}Cre}$ mice were massively enlarged (Fig. 5 C) and consisted mainly of ITK-SYK–expressing TCR-β$^+$ and eGFP$^+$ T cells with an activated phenotype (Fig. 5 D and not depicted; n = 40 mice analyzed). Histological analysis revealed a complete disruption of the normal spleen architecture by a diffuse infiltrate of medium- to large-sized lymphoid cells that exhibited irregular nuclei, prominent nucleoli, and high mitotic rates strongly suggestive of a neoplastic growth (Fig. 6 A). Ki-67 staining further demonstrated a high proliferation (Fig. 6 A). The abnormal T cell populations were primarily CD4$^+$ in ~61% of the animals (Type I), predominantly CD8$^+$ in 23% (Type II), and a mix of CD4$^+$ and CD8$^+$ T cells in the remaining mice (Type III; Fig. 6 B). The atypical lymphoid cells always infiltrated the bone marrow (Fig. 6 C) and grew invasively into solid organs, including kidneys, livers, and lungs (Fig. 6 D). Immunohistochemical analysis with anti-CD3 antibodies confirmed the T cell nature of the infiltrate (Fig. 6 D). To characterize clonality, we analyzed their TCR-Vβ chain repertoire by flow cytometry (Fig. 6 E). The repertoire was always skewed and consistently enriched for individual TCR-Vβ clones (n = 33 mice analyzed). Although the specifically expanded TCR-Vβ chain clones differed among distinct animals, we regularly observed that the identical T cell clones infiltrated all tested tissues in one individual mouse. To further study T cell clonality, we performed a PCR-based and computer-assisted fragment length analysis (Genescan) for TCR-β and TCR-γ locus gene rearrangements (Kneba et al., 1995; van Dongen et al., 2003). Clonal TCR rearrangements were detected in all tested diseased ITK-SYK$^{CD4\text{-}Cre}$ (n = 3) but not in CD4-Cre control mice (n = 4; Fig. 6 F and not depicted).

Finally, we tested whether ITK-SYK–induced T cell tumors could be transplanted. To this end, we injected ITK-SYK–expressing T cells from affected animals intravenously into recipient mice. Tail blood analysis documented that the transplanted cells could massively expand in the recipients (Fig. 7 A). Morphological and flow cytometric analyses again revealed a lethal infiltration into lymphoid and nonlymphoid organs that was identical to the original disease (Fig. 7, B–D). Thus, enforced ITK-SYK expression in the T cell lineage induces a highly aggressive transplantable T cell lymphoma with a malignant growth pattern that resembles the clinical and pathological features of human PTCL (Cotta and Hsi, 2008).

analyzed. (E) Selective expansion of distinct T cell clones. Single cell suspensions from spleen (SPL), kidney (KID), and liver (LIV) of three individual mice were stained with antibodies against CD4, CD8, and a panel of TCR-Vβ chain–specific antibodies (see Materials and methods). Frequencies of CD4$^+$ or CD8$^+$ cells expressing the indicated TCR-Vβ chains in the spleen of control mice (open histograms) or frequencies of cells expressing the indicated TCR-Vβ chains in spleen, kidney, and liver from diseased ITK-SYK$^{CD4\text{-}Cre}$ mice (gray histograms) are shown. (F) Genescan analysis for TCR gene rearrangements. Representative fragment size distributions of fluorochrome-labeled PCR products of the Dβ2/Jβ2 junction of a control and a diseased ITK-SYK$^{CD4\text{-}Cre}$ mouse are shown. Data shown are representative of three mice per genotype analyzed. Data in A–F are from ITK-SYK$^{CD4\text{-}Cre}$ mice that were older than 12 wk and showed disease symptoms.

ITK-SYK expression in single T cells is able to induce T cell lymphomas in ITK-SYK$^{CD19\text{-}Cre}$ mice

Human cancers do not arise from oncogene expression throughout an entire cell lineage but are caused by somatic mutations in single tumor cell precursors. Surprisingly, we observed that all ITK-SYK$^{CD19\text{-}Cre}$ mice eventually also developed a lethal wasting syndrome (Fig. 8 A) with splenomegaly (Fig. 8 B) and infiltration of abnormal lymphocytes into multiple organs (Fig. 8, C and D). Although the CD19-Cre transgene induces very efficient and highly selective ITK-SYK expression in the B cell lineage (Fig. 2, C and D; and Fig. 4), the lymphomas in ITK-SYK$^{CD19\text{-}Cre}$ mice were, intriguingly, all of T cell origin and macroscopically and microscopically indistinguishable from the T cell lymphomas in ITK-SYK$^{CD4\text{-}Cre}$ mice. They consisted of enlarged, activated, and highly proliferative Ki-67$^+$ and TCR-β$^+$ ITK-SYK–expressing cells (Fig. 8, C–E; and not depicted), which could transmit the disease to recipients in transplantation experiments (not depicted). However, in contrast to ITK-SYK$^{CD4\text{-}Cre}$ mice we never observed mixed CD4$^+$ and CD8$^+$ infiltrates in ITK-SYK$^{CD19\text{-}Cre}$ mice but, instead, always homogenous tumor cell populations that express either CD4, in 75% of the cases (Type I), or CD8 (Type II; Fig. 8 F) and which were of clonal origin, as determined by surface staining for TCR-Vβ chains (Fig. 8 G; $n = 12$) or Genescan analysis ($n = 5$; not depicted). We therefore conclude that a rare and untypical expression of ITK-SYK in the T cell lineage of ITK-SYK$^{CD19\text{-}Cre}$ mice, presumably as a result of "leaky" Cre expression, is able to drive neoplastic transformation and malignant expansion of single T cell clones, which closely models the pathophysiological situation in human PTCL patients.

DISCUSSION

Chromosomal translocations in hematological malignancies have always provided key insights into disease pathogenesis. Although some specific translocations are rare, the signaling pathways that are deregulated by these events are regularly hit by alternative genetic mechanisms such as mutations or amplifications in translocation negative cases or other tumor subentities (Fröhling and Döhner, 2008). As these aberrant signals directly trigger tumorigenesis they constitute rational targets for therapeutic interventions.

We demonstrate that the human PTCL-associated fusion tyrosine kinase ITK-SYK triggers molecular and cellular features of strong TCR signaling in vitro and in vivo. These events include tyrosine phosphorylation of TCR-proximal proteins, activation of downstream cascades, and functional outcomes that, similar to normal antigen receptor signaling, depend on the cellular context. Examples are deletion of DP thymocytes or activation of T cells in the periphery. Therefore, our results indicate that ITK-SYK acts as an intracellular mimic of a strong antigen receptor signal. Yet ITK-SYK signaling is certainly not identical to ligand-induced TCR signaling and differs in terms of kinetics and some quantitative aspects like induction of maximal IL-2 production. Moreover, normal TCR signaling is regularly terminated at the end of an immune response, whereas ITK-SYK signaling is chronic. Ultimately, ITK-SYK induces highly malignant PTCLs with 100% penetrance. The fact that the tumors are clonal suggests that cooperating events contribute to proliferative advantage and outgrowth of individual lymphoma cell clones. Notably, sporadic ITK-SYK expression in single T cells of ITK-SYK$^{CD19\text{-}Cre}$ mice drives oncogenesis, indicating that ITK-SYK is a bona fide oncogene. Secondary oncogenic events

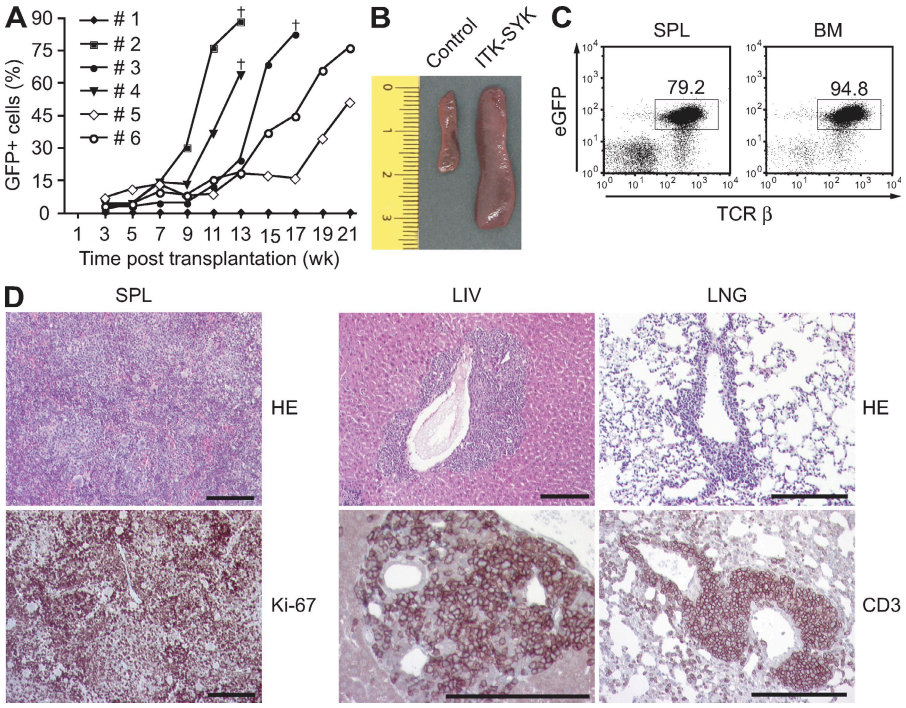

Figure 7. Proliferation and infiltration of ITK-SYK–expressing T cells upon transplantation. (A) Splenic cells from diseased ITK-SYK$^{CD4\text{-}Cre}$ animals older than 12 wk of age were intravenously injected into nude recipient mice for transplantation. The frequencies of ITK-SYK–expressing eGFP$^+$ peripheral blood cells in the recipients were monitored over time. Recipients that succumbed to the disease are indicated (†). Representative examples are shown. 9 out of 10 donor mice transplanted the disease. Five independent transplantations were performed. (B) Spleens from a control and a representative recipient mouse from A are shown (in centimeters). (C) Recipients were sacrificed upon signs of disease, and bone marrow (BM) and spleen (SPL) suspensions were stained against TCR-β. Representative frequencies of eGFP fluorescent T cells in spleen and bone marrow of 10 analyzed diseased recipients are indicated. (D) Tissue sections from spleen (SPL), liver (LIV), and lung (LNG) were analyzed after H&E staining or immunohistochemistry with anti-CD3 or anti-Ki-67 antibodies. Bars, 1 mm. Representative examples of four analyzed diseased recipients are shown.

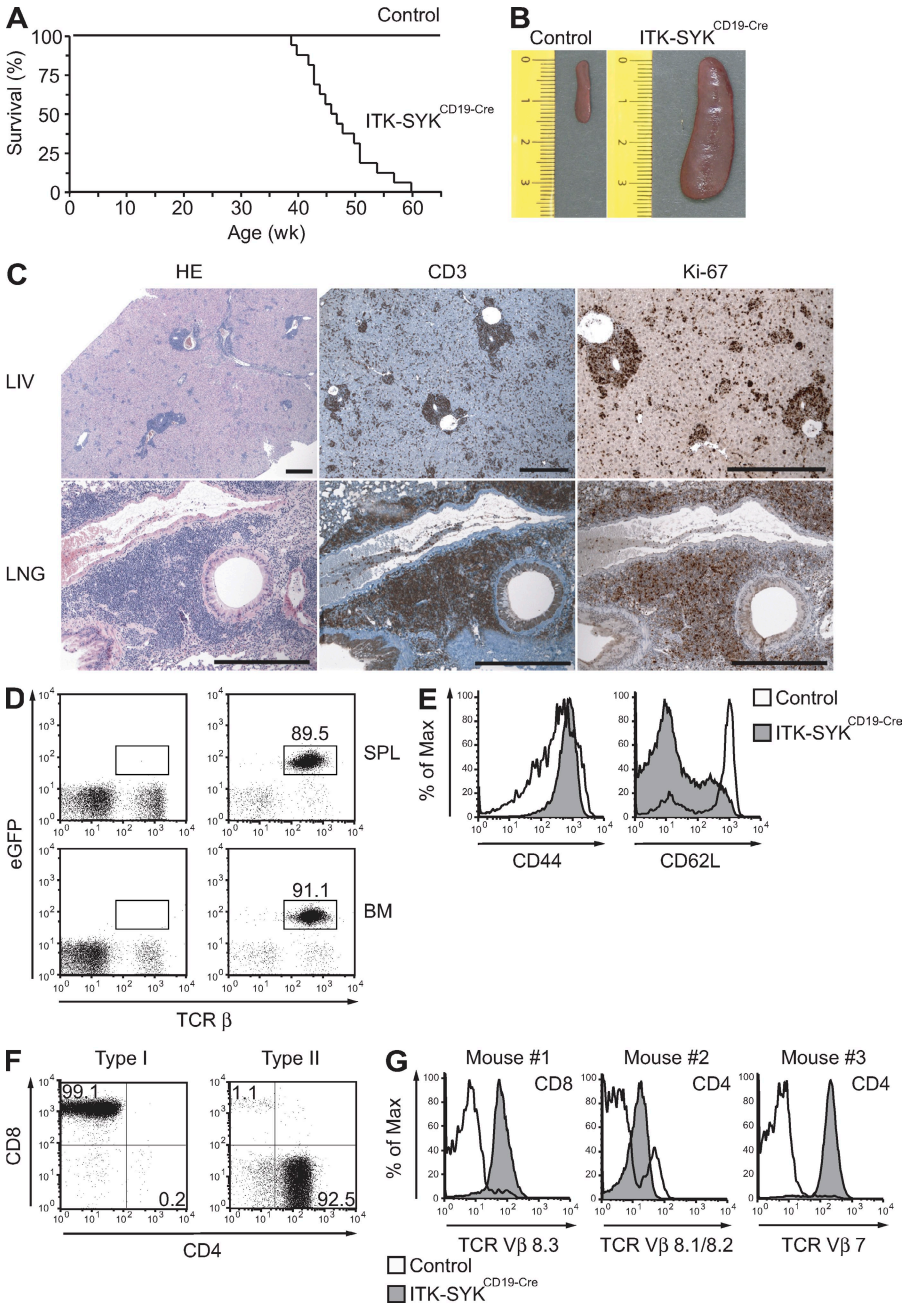

Figure 8. ITK-SYK$^{CD19\text{-}Cre}$ mice develop clonal PTCLs. (A) ITK-SYK$^{CD19\text{-}Cre}$ mice succumb to disease. Kaplan-Meier curve of ITK-SYK$^{CD19\text{-}Cre}$ (n = 18) and control (CD19-Cre) mice (n = 10). (B) Splenomegaly in ITK-SYK$^{CD19\text{-}Cre}$ mice. Representative spleens from 50-wk-old control and ITK-SYK$^{CD19\text{-}Cre}$ mice are shown (in centimeters). (C) Solid organ infiltration with abnormally proliferating T cells in ITK-SYK$^{CD19\text{-}Cre}$ mice. H&E staining and immunohistochemistry with anti-CD3 and anti-Ki-67 antibodies were performed on liver (LIV) and lung (LNG) sections. Bars, 1 mm. Data representative of six diseased ITK-SYK$^{CD19\text{-}Cre}$ mice are shown. (D) Bone marrow (BM) or spleen (SPL) cell suspensions of 50-wk-old control and ITK-SYK$^{CD19\text{-}Cre}$ mice were stained against TCR-β. The frequency of eGFP$^+$ T cells in a representative ITK-SYK$^{CD19\text{-}Cre}$ mouse is indicated. (E) Expanded T cells in ITK-SYK$^{CD19\text{-}Cre}$ mice display an activated phenotype. CD44 and CD62L surface expression on affected T cells or controls was assessed using FACS. One representative example of CD4$^+$ T cells is shown. (F) Spleen cells from diseased ITK-SYK$^{CD19\text{-}Cre}$ mice (n = 16) were stained against CD4 and CD8. Examples of preferential CD4$^+$ T cell (Type I) or CD8$^+$ T cell (Type II) expansions are shown. (G) T cell populations in ITK-SYK$^{CD19\text{-}Cre}$ mice are clonal. Single cell suspensions from spleens of individual mice were stained with antibodies against CD4, CD8, and a panel of antibodies against TCR-Vβ chains (see Materials and methods). Frequencies of CD4$^+$ or CD8$^+$ cells expressing the indicated TCR-Vβ chains in control (open histograms) or diseased ITK-SYK$^{CD19\text{-}Cre}$ (gray histograms) mice are shown. Data in B and D–G are representative of six independent experiments with a total number of at least 10 mice analyzed per genotype are shown. If not indicated otherwise, all panels show data from ITK-SYK$^{CD19\text{-}Cre}$ mice that were older than 40 wk and showed disease symptoms.

might also contribute to lymphoma development in ITK-SYK$^{CD19\text{-}Cre}$ mice.

Although the ITK-SYK fusion kinase is only found in a subset of PTCL patients (Streubel et al., 2006), a recent study with >140 PTCL samples reported aberrant expression of activated SYK in >90% of the cases (Feldman et al., 2008). Moreover, PTCL cells regularly exhibit characteristics of activated T cells including their gene expression signatures (Piccaluga et al., 2007; Savage, 2007). Together with our experimental results, these clinical findings suggest that an aberrant activation of antigen receptor signaling pathways could be a common driver of PTCL pathogenesis.

Antigen-mediated TCR ligation induces a recruitment of the SYK family member ZAP-70 to the receptor complex for LAT and SLP-76 phosphorylation and subsequent cell activation (Samelson, 2002). ITK-SYK is constitutively associated with lipid rafts and, as such, is presumably in constant proximity to its key substrates. The localization of ITK-SYK into the proper T cell microdomains is mediated via the PH domain and also potentially via the TH domain, which both originate from the T cell kinase ITK (Berg et al., 2005). These protein modules are known to coordinate membrane localization and binding to SLP-76 and LAT in a remarkably selective manner, as ITK does not efficiently interact with related B cell molecules including

SLP-65 (Hashimoto et al., 1999; Su et al., 1999; Bunnell et al., 2000). This might explain why B cell–intrinsic expression of ITK-SYK has no apparent effects in the B cell lineage. Consistent with our findings, ITK-SYK kinase activity and membrane localization are also required for ITK-SYK–mediated transformation of an immortalized fibroblast cell line in vitro (Rigby et al., 2009). Together, these results suggest that therapeutic strategies for ITK-SYK inhibition could either target the ITK-SYK kinase activity or try to interfere with ITK-SYK localization. Our experiments in Jurkat cells demonstrated that the SYK kinase inhibitor R406 can very potently block ITK-SYK signaling. Still, it is currently unclear whether constitutive ITK-SYK signaling is predominantly responsible for tumor initiation or also essential for disease maintenance. Thus, studies are necessary that investigate the responsiveness of ITK-SYK–induced lymphoma to R406 treatment in vivo.

Aberrant antigen receptor signaling is frequently observed in human lymphoid malignancies beyond PTCL. Chronic active BCR signaling was recently described in diffuse large B cell lymphomas (Davis et al., 2010). Other lymphoma entities with aberrant activities of antigen receptor signaling pathways are chronic lymphocytic leukemias, which regularly show aberrant ZAP-70 expression, mucosa-associated lymphoid tissue lymphomas, which often develop in the context of chronic antigenic stimulation, or follicular lymphoma (Küppers, 2005). Our study provides in vivo evidence that constitutively enforced antigen receptor signals are directly able to induce oncogenesis. The downstream signaling cascades that are critical for lymphoma initiation or maintenance are not well defined. The presented mouse models will serve as valuable tools to genetically dissect these pathways in vivo. Finally, in addition to the mentioned SYK inhibitor, several small molecule drugs, which interfere with antigen receptor signaling, are already available or are in preclinical or clinical development for malignant or nonmalignant immune-mediated diseases. Our clinically relevant PTCL model will help to identify compounds that could be of potential use for the treatment of PTCLs. In light of the minimal effectiveness of conventional chemotherapy in PTCL treatment such studies are urgently warranted.

MATERIALS AND METHODS

Animals. Human ITK-SYK cDNA (Streubel et al., 2006) was cloned into a Rosa26 targeting vector (Sasaki et al., 2006), linearized, and electroporated into E14K embryonic stem cells as previously described (Ruland et al., 2001). Successful homologous recombination at the Rosa26 locus was confirmed by standard Southern blot analysis using a 5′ flanking probe as previously described (Ruland et al., 2001). Blastocyst injection of two independent clones and subsequent chimera breeding resulted in $Rosa26^{loxSTOPlox\text{-}ITK\text{-}SYK}$ mice. $Rosa26^{loxSTOPlox\text{-}ITK\text{-}SYK}$ mice were crossed with either CD4-Cre (Lee et al., 2001) or CD19-Cre mice (Rickert et al., 1997). Littermates were used in all subsequent experiments. Athymic *Foxn1*$^{nu/nu}$ mice purchased from Harlan were used as recipients in transplantation experiments. Studies were conducted according to federal and institutional guidelines. Animal protocols were approved by the government of Upper Bavaria.

Retroviral expression vectors. Retroviral constructs were generated by cloning ITK-SYK, ITK-SYK (K262R) (ITK-SYK^{KD}), or ITK-SYK (R29C) (ITK-SYK^{PHmut}) cDNA into IRES GFP containing MSCV-based vectors using standard molecular biology techniques as previously described (Grundler et al., 2005). Retroviral particles were generated upon transfection of Phoenix-E packaging cells as previously described (Grundler et al., 2005).

Cell culture. Jurkat cells were cultured in RPMI-1640 medium supplemented with 10% fetal bovine serum. Phoenix-E packaging cells were maintained in DME supplemented with 10% fetal bovine serum. The SYK inhibitor R406 (Rigel Pharmaceuticals) was used at a final concentration of 2 μM where indicated.

ELISA. Cell supernatants from Jurkat cells were harvested 36 h after retroviral infection and CD3 (10 μg/ml)/CD28 (2 μg/ml) stimulation as indicated. IL-2 concentrations were determined via ELISA (OptEIA Human IL-2 ELISA Set; BD).

T and B cell purification. For protein analysis, T or B cells from spleen or lymph nodes were isolated by negative selection with magnetic beads (Dynabeads; Invitrogen) and antibodies against CD11b, B220, or Thy1.2 as previously described (Ferch et al., 2007).

Lipid raft preparation. 10^7 Jurkat cells or 5×10^7 purified lymphocytes per assay point were kept unstimulated or stimulated with 5 μg/ml CD3/1 μg/ml CD28 for 5 min as indicated and subsequently lysed in Brij lysis buffer as previously described (Ferch et al., 2007). Mice older than 12 wk were used for T cell preparations to obtain sufficient numbers of ITK-SYK–expressing T lymphocytes. Postnuclear supernatants were mixed with 85% (wt/vol) sucrose, overlaid with 35% (wt/vol) and 5% (wt/vol) sucrose, and separated by ultracentrifugation. Lipid raft and cytoplasmatic fractions were analyzed for the presence of the lipid raft marker GM1 (Ferch et al., 2007).

Western blot analysis. For whole cell protein analysis, Jurkat cells or primary lymphocytes were lysed with CHAPS buffer and subsequently subjected to Western blot analysis as previously described (Ferch et al., 2007). Alternatively, lipid raft or nonraft fractions were analyzed. The following antibodies were used: anti-Emt (2F12; mouse monoclonal; Santa Cruz Biotechnology, Inc.) for ITK or ITK-SYK detection, anti–phospho-tyrosine (P-Tyr-100; mouse monoclonal; Cell Signaling Technology), anti–phospho-PLCγ1 (Tyr783; rabbit polyclonal; Cell Signaling Technology), and anti-β-actin (20–33; Sigma-Aldrich).

Flow cytometry. FACS analysis was performed using standard protocols (Ferch et al., 2007). In brief, Jurkat cells were either surface stained with anti-human CD69 antibody or intracellularly stained after permeabilization with 70% ice-cold methanol with antibodies against phosphorylated forms of SLP-76 (pY128), LAT (pY171), PLCγ1 (pY783), AKT (pS473), ERK1/2 (pT202/pY204), or p38 (pT180/pY182). Primary cell suspensions from thymus, spleen, lymph nodes, bone marrow, or peripheral blood were directly labeled. Single cell suspensions from liver, kidney, or lung were first purified by Percoll gradient centrifugation. Fluorescently labeled antibodies against the following surface proteins were used for mouse cell staining: B220 (RA3_6B2); TCR-β (H57-597); CD3 (1452C11); CD4 (Gk1.5); CD5 (53–7.3); CD8 (53–6.7); CD21/35 (7G6); CD23 (B3B4); CD44 (IM7); CD62L (MEK-14); CD86 (GL1); IgM (II/41), Vβ3-TCR (KJ25), Vβ4-TCR (CTVB4), Vβ6-TCR (RR4-7), Vβ7-TCR (TR310), Vβ8.1/8.2-TCR (MR5-2), Vβ8.3-TCR (CT-8C1), Vβ10b-TCR (CTVB10b), Vβ11-TCR (CTVB11), and Vβ12b-TCR (CTVB12b). Data were acquired on a FACSCalibur or FACSCanto II flow cytometer (BD). FlowJo Software (Tree Star, Inc.) was used for data analysis.

Histology. All organs were fixed in 4% formaldehyde and paraffin embedded. 3–5-μm-thick sections were cut and stained with H&E. Immunohistochemistry was performed on an automated immunostainer (Ventana Medical Systems, Inc.) according to the company's protocols for open procedures with slight modifications. The antibody panel used included CD3 (SP7; Thermo Fisher Scientific), B220 (BD), Ki-67 (SP6; Thermo Fisher Scientific),

and cleaved Caspase 3 (ASP 175; Cell Signaling Technology). Appropriate positive controls were used to confirm the adequacy of the staining.

Genescan analysis. Genomic DNA was extracted from total splenic cell suspensions of diseased ITK-SYK$^{CD4\text{-}Cre}$, ITK-SYK$^{CD19\text{-}Cre}$, or control mice (CD4-Cre or CD19-Cre, respectively). V-D-J and incomplete D-J rearrangements of the TCR-β locus were analyzed via five individual PCR reactions with the following primer combinations: Vβ(1–20)-Jβ1, Vβ(1–20)-Jβ2, Dβ1-Jβ1, Dβ2-Jβ2, and Dβ1-Jβ2. Primer sets consisted of a mixture of 20 family-specific upstream primers located within the Vβ gene segments or consensus primers immediately located 5′ of the Dβ1/Dβ2 rearrangement and 5′FAM-labeled consensus primers immediately located 3′ of the Jβ1/Jβ2 rearrangement as previously described (Gärtner et al., 1999). TCR-γ locus rearrangement was analyzed with a PCR reaction using a Vγ4 and a 5′-FAM–labeled Jγ1 consensus primer as described (Kawamoto et al., 2000). 5′-FAM–labeled PCR products were size separated by capillary POP-7-Polymer electrophoresis and visualized via automated scanning by using a 3700 Genetic Analyzer (Applied Biosystems). Reagents were all obtained from Applied Biosystems. Fragment size distribution was determined by GeneMapper software (Applied Biosystems) and analyzed as previously described (Kneba et al., 1995; van Dongen et al., 2003).

Transplantation. 6-wk-old athymic *Foxn1*$^{nu/nu}$ mice (Harlan) were intravenously injected with 1.5×10^7 splenocytes isolated from diseased ITK-SYK$^{CD4\text{-}Cre}$ or ITK-SYK$^{CD19\text{-}Cre}$ mice. Recipients were monitored daily for signs of disease and blood samples were analyzed by FACS at the indicated time points.

Statistical analysis. Where indicated, results were analyzed for statistical significance with the unpaired two-tailed Student's *t* test. Differences between groups were considered as significant at p-values <0.05.

Online supplemental material. Fig. S1 shows results from phosflow experiments investigating the phosphorylation status of TCR signaling molecules upon CD3/CD28 stimulation in retrovirally infected Jurkat cells. Fig. S2 presents the immunohistochemical expression analysis of CD3, Ki-67, and the active form of Caspase 3 (Caspase 3A) in spleen sections from of 4–5-wk-old ITK-SYK$^{CD4\text{-}Cre}$ or control CD4-Cre animals. Online supplemental material is available at http://www.jem.org/cgi/content/full/jem.20092042/DC1.

We thank Marc Schmidt-Supprian for plasmids and helpful discussions, Rigel Inc. for providing the SYK inhibitor R406, Stefan Wanninger, Vera Pfänder, Claudia Kloss, and Susanne Weiss for cloning and excellent technical assistance, and Gisela Keller for access to gene scan equipment.

This work was supported by Sonderforschungsbereich grants from Deutsche Forschungsgemeinschaft to L. Quintanilla-Martinez and J. Ruland and by a Max-Eder-Program grant from Deutsche Krebshilfe to J. Ruland.

The authors have no conflicting financial interests.

Submitted: 21 September 2009
Accepted: 12 March 2010

REFERENCES

Abraham, R.T., and A. Weiss. 2004. Jurkat T cells and development of the T-cell receptor signalling paradigm. *Nat. Rev. Immunol.* 4:301–308. doi:10.1038/nri1330

Berg, L.J., L.D. Finkelstein, J.A. Lucas, and P.L. Schwartzberg. 2005. Tec family kinases in T lymphocyte development and function. *Annu. Rev. Immunol.* 23:549–600. doi:10.1146/annurev.immunol.22.012703.104743

Bunnell, S.C., M. Diehn, M.B. Yaffe, P.R. Findell, L.C. Cantley, and L.J. Berg. 2000. Biochemical interactions integrating Itk with the T cell receptor-initiated signaling cascade. *J. Biol. Chem.* 275:2219–2230. doi:10.1074/jbc.275.3.2219

Cotta, C.V., and E.D. Hsi. 2008. Pathobiology of mature T-cell lymphomas. *Clin. Lymphoma Myeloma.* 8:S168–S179. doi:10.3816/CLM.2008.s.013

Davis, R.E., V.N. Ngo, G. Lenz, P. Tolar, R.M. Young, P.B. Romesser, H. Kohlhammer, L. Lamy, H. Zhao, Y. Yang, et al. 2010. Chronic active B-cell-receptor signalling in diffuse large B-cell lymphoma. *Nature.* 463:88–92. doi:10.1038/nature08638

Dykstra, M., A. Cherukuri, H.W. Sohn, S.J. Tzeng, and S.K. Pierce. 2003. Location is everything: lipid rafts and immune cell signaling. *Annu. Rev. Immunol.* 21:457–481. doi:10.1146/annurev.immunol.21.120601.141021

Escalón, M.P., N.S. Liu, Y. Yang, M. Hess, P.L. Walker, T.L. Smith, and N.H. Dang. 2005. Prognostic factors and treatment of patients with T-cell non-Hodgkin lymphoma: the M. D. Anderson Cancer Center experience. *Cancer.* 103:2091–2098. doi:10.1002/cncr.20999

Feldman, A.L., D.X. Sun, M.E. Law, A.J. Novak, A.D. Attygalle, E.C. Thorland, S.R. Fink, J.A. Vrana, B.L. Caron, W.G. Morice, et al. 2008. Overexpression of Syk tyrosine kinase in peripheral T-cell lymphomas. *Leukemia.* 22:1139–1143. doi:10.1038/leu.2008.77

Ferch, U., C.M. zum Büschenfelde, A. Gewies, E. Wegener, S. Rauser, C. Peschel, D. Krappmann, and J. Ruland. 2007. MALT1 directs B cell receptor-induced canonical nuclear factor-kappaB signaling selectively to the c-Rel subunit. *Nat. Immunol.* 8:984–991. doi:10.1038/ni1493

Friedberg, J.W., J. Sharman, J. Sweetenham, P.B. Johnston, J.M. Vose, A. Lacasce, J. Schaefer-Cutillo, S. De Vos, R. Sinha, J.P. Leonard, et al. 2010. Inhibition of Syk with fostamatinib disodium has significant clinical activity in non-Hodgkin lymphoma and chronic lymphocytic leukemia. *Blood.* 115:2578–2585. doi:10.1182/blood-2009-08-236471

Fröhling, S., and H. Döhner. 2008. Chromosomal abnormalities in cancer. *N. Engl. J. Med.* 359:722–734. doi:10.1056/NEJMra0803109

Gärtner, F., F.W. Alt, R. Monroe, M. Chu, B.P. Sleckman, L. Davidson, and W. Swat. 1999. Immature thymocytes employ distinct signaling pathways for allelic exclusion versus differentiation and expansion. *Immunity.* 10:537–546. doi:10.1016/S1074-7613(00)80053-9

Grundler, R., C. Miething, C. Thiede, C. Peschel, and J. Duyster. 2005. FLT3-ITD and tyrosine kinase domain mutants induce two distinct phenotypes in a murine bone marrow transplantation model. *Blood.* 105:4792–4799. doi:10.1182/blood-2004-11-4430

Hashimoto, S., A. Iwamatsu, M. Ishiai, K. Okawa, T. Yamadori, M. Matsushita, Y. Baba, T. Kishimoto, T. Kurosaki, and S. Tsukada. 1999. Identification of the SH2 domain binding protein of Bruton's tyrosine kinase as BLNK—functional significance of Btk-SH2 domain in B-cell antigen receptor-coupled calcium signaling. *Blood.* 94:2357–2364.

Kawamoto, H., T. Ikawa, K. Ohmura, S. Fujimoto, and Y. Katsura. 2000. T cell progenitors emerge earlier than B cell progenitors in the murine fetal liver. *Immunity.* 12:441–450. doi:10.1016/S1074-7613(00)80196-X

Kneba, M., I. Bolz, B. Linke, and W. Hiddemann. 1995. Analysis of rearranged T-cell receptor beta-chain genes by polymerase chain reaction (PCR) DNA sequencing and automated high resolution PCR fragment analysis. *Blood.* 86:3930–3937.

Küppers, R. 2005. Mechanisms of B-cell lymphoma pathogenesis. *Nat. Rev. Cancer.* 5:251–262. doi:10.1038/nrc1589

Lee, P.P., D.R. Fitzpatrick, C. Beard, H.K. Jessup, S. Lehar, K.W. Makar, M. Pérez-Melgosa, M.T. Sweetser, M.S. Schlissel, S. Nguyen, et al. 2001. A critical role for Dnmt1 and DNA methylation in T cell development, function, and survival. *Immunity.* 15:763–774. doi:10.1016/S1074-7613(01)00227-8

Myung, P.S., N.J. Boerthe, and G.A. Koretzky. 2000. Adapter proteins in lymphocyte antigen-receptor signaling. *Curr. Opin. Immunol.* 12:256–266. doi:10.1016/S0952-7915(00)00085-6

Palacios, E.H., and A. Weiss. 2007. Distinct roles for Syk and ZAP-70 during early thymocyte development. *J. Exp. Med.* 204:1703–1715. doi:10.1084/jem.20070405

Piccaluga, P.P., C. Agostinelli, A. Califano, M. Rossi, K. Basso, S. Zupo, P. Went, U. Klein, P.L. Zinzani, M. Baccarani, et al. 2007. Gene expression analysis of peripheral T cell lymphoma, unspecified, reveals distinct profiles and new potential therapeutic targets. *J. Clin. Invest.* 117:823–834. doi:10.1172/JCI26833

Rickert, R.C., J. Roes, and K. Rajewsky. 1997. B lymphocyte-specific, Cre-mediated mutagenesis in mice. *Nucleic Acids Res.* 25:1317–1318. doi:10.1093/nar/25.6.1317

Rigby, S., Y. Huang, B. Streubel, A. Chott, M.Q. Du, S.D. Turner, and C.M. Bacon. 2009. The lymphoma-associated fusion tyrosine kinase ITK-SYK requires pleckstrin homology domain-mediated membrane localization for activation and cellular transformation. *J. Biol. Chem.* 284:26871–26881. doi:10.1074/jbc.M109.034272

Ruland, J., G.S. Duncan, A. Elia, I. del Barco Barrantes, L. Nguyen, S. Plyte, D.G. Millar, D. Bouchard, A. Wakeham, P.S. Ohashi, and T.W. Mak. 2001. Bcl10 is a positive regulator of antigen receptor-induced activation of NF-kappaB and neural tube closure. *Cell.* 104:33–42. doi:10.1016/S0092-8674(01)00189-1

Sada, K., T. Takano, S. Yanagi, and H. Yamamura. 2001. Structure and function of Syk protein-tyrosine kinase. *J. Biochem.* 130:177–186.

Samelson, L.E. 2002. Signal transduction mediated by the T cell antigen receptor: the role of adapter proteins. *Annu. Rev. Immunol.* 20:371–394. doi:10.1146/annurev.immunol.20.092601.111357

Sasaki, Y., E. Derudder, E. Hobeika, R. Pelanda, M. Reth, K. Rajewsky, and M. Schmidt-Supprian. 2006. Canonical NF-kappaB activity, dispensable for B cell development, replaces BAFF-receptor signals and promotes B cell proliferation upon activation. *Immunity.* 24:729–739. doi:10.1016/j.immuni.2006.04.005

Savage, K.J. 2007. Peripheral T-cell lymphomas. *Blood Rev.* 21:201–216. doi:10.1016/j.blre.2007.03.001

Sebzda, E., S. Mariathasan, T. Ohteki, R. Jones, M.F. Bachmann, and P.S. Ohashi. 1999. Selection of the T cell repertoire. *Annu. Rev. Immunol.* 17:829–874. doi:10.1146/annurev.immunol.17.1.829

Streubel, B., U. Vinatzer, M. Willheim, M. Raderer, and A. Chott. 2006. Novel t(5;9)(q33;q22) fuses ITK to SYK in unspecified peripheral T-cell lymphoma. *Leukemia.* 20:313–318. doi:10.1038/sj.leu.2404045

Su, Y.W., Y. Zhang, J. Schweikert, G.A. Koretzky, M. Reth, and J. Wienands. 1999. Interaction of SLP adaptors with the SH2 domain of Tec family kinases. *Eur. J. Immunol.* 29:3702–3711. doi:10.1002/(SICI)1521-4141(199911)29:11<3702::AID-IMMU3702>3.0.CO;2-R

van Dongen, J.J., A.W. Langerak, M. Brüggemann, P.A. Evans, M. Hummel, F.L. Lavender, E. Delabesse, F. Davi, E. Schuuring, R. García-Sanz, et al. 2003. Design and standardization of PCR primers and protocols for detection of clonal immunoglobulin and T-cell receptor gene recombinations in suspect lymphoproliferations: report of the BIOMED-2 Concerted Action BMH4-CT98-3936. *Leukemia.* 17:2257–2317. doi:10.1038/sj.leu.2403202

Weinblatt, M.E., A. Kavanaugh, R. Burgos-Vargas, A.H. Dikranian, G. Medrano-Ramirez, J.L. Morales-Torres, F.T. Murphy, T.K. Musser, N. Straniero, A.V. Vicente-Gonzales, and E. Grossbard. 2008. Treatment of rheumatoid arthritis with a Syk kinase inhibitor: a twelve-week, randomized, placebo-controlled trial. *Arthritis Rheum.* 58:3309–3318. doi:10.1002/art.23992